

## INFLUENCE OF ANNEALING TEMPERATURE ON THE GROWTH OF SPIN COATED $Mn_3O_4$ THIN FILMS FROM THE DECOMPOSITION OF BIS(N-CYCLOHEXYL-SALICYDENAMINATO)MANGANESE(II) COMPLEX

T. XABA\*, N. D. SHOOTO

*Department of Chemistry, Vaal University of Technology, P/Bag X021, Vanderbijlpark, South Africa*

The preparation of *bis*(N-cyclohexyl-salicydenaminato)manganese(II) complex as a precursor for the fabrication of  $Mn_3O_4$  nanocrystalline thin films is reported. The manganese oxide thin films were chemically deposited on glass and silicon substrates by spin-coating and effect of the annealing temperature on the thin films has been systemically investigated. The optical absorption and emission spectra of all the  $Mn_3O_4$  thin films were red-shifted when the temperature was raised. The optical band gap energies were determined and found to be decreasing as the annealing temperature was increasing. X-ray diffraction patterns confirmed the formation of tetragonal phase structures with lattice parameters of  $a = b = 5.75 \text{ \AA}$  and  $c = 9.44 \text{ \AA}$ . SEM micrograms disclosed an improvement in crystallinity of the particles on the surface of the substrate when the temperature was increased.

(Received June 18, 2020; Accepted February 3, 2021)

*Keywords:* Manganese complex, Manganese oxide, Thin films, Substrates

### 1. Introduction

Recently, the synthesis of metal oxide nanomaterials has gained tremendous interest due to their many scientific applications and since they are easily employed in technological systems such as solar cells, sensors, catalysis etc [1-3]. Among various kinds of metal oxide, manganese oxides materials have invented considerable scientific and technological interest due to their electronic and magnetic properties [4]. Manganese oxide is a transition metal oxide and an important functional oxide that have features such as mixed valence. It is also an important member of the family ( $MnO$ ,  $Mn_3O_4$ ,  $Mn_2O_3$ ,  $Mn_5O_8$  and  $MnO_2$ ) that exhibits distinct chemical and physical properties [5]. Manganese oxide materials can be applied in numerous fields such as in oxidation processes [6], batteries [7], catalysis [8], ion exchanges [9] etc.

Hausmannite,  $Mn_3O_4$ , is one of the most stable member of manganese oxide family and has normal structure with a tetragonal distortion along the C-axis [10, 11].  $Mn_3O_4$  has important electrical and magnetic properties as giant magnetoresistance, and metal-insulator transition materials [12,13].  $Mn_3O_4$  has gained interest in many industrial and technological applications such as water oxidation [14], electrochemical material [15], humidity sensors [16], rechargeable lithium batteries [17] and catalytic materials for the oxidative destruction of volatile organic compounds [18]. Numerous techniques have been reported for the preparation of  $Mn_3O_4$  thin films. These methods may include dip coating [19], atomic layer deposition [20], molecular beam epitaxy [21], electrochemical deposition [22], pulsed laser deposition [23], chemical bath deposition [24], electrostatic spray deposition [25], metal organic chemical vapour deposition [26]. Xu *et al.* [27] have reported the preparation and characterization of hausmannite  $Mn_3O_4$  thin films on the glass substrate through chemical bath deposition using a low temperature. They discovered that the floating substrate was giving high-quality thin films during the CBD procedure. The study based on the preparation of manganese (II) precursor for the deposition of  $MnF_2$  or  $Mn_3O_4$  via the metal organic chemical vapour deposition (MOCVD) was reported Catalano and Malandrino [28].

---

\* Corresponding author: thokozanix@vut.ac.za

Manganese difluoride nano-rod were attained under atmospheric pressure, while the hausmannite  $\text{Mn}_3\text{O}_4$  films were achieved under reduced pressure.

Among the synthetic techniques for the making of thin films, spin coating method has been regarded as the most suitable technique since it is cost effective, fast and simple method to use for the deposition of thin film. It produces films that are highly uniform and homogeneous [29]. In this work, the preparation of *bis*(N-cyclohexyl-1-salicydenaminato)manganese(II) complex from the reaction of a primary amine, Schiff base ligand, and manganese acetate is reported. The precursor was dissolved in tetrahydrofuran and then transferred onto the glass and silicon substrates to make the films through spin coater. The films were annealed at various temperatures to make  $\text{Mn}_3\text{O}_4$  thin films. The formation of the precursor was confirmed with Fourier transform infrared (FTIR) spectroscopy and elemental analysis. The thermal properties of the precursor were studied with thermogravimetric (TGA) analysis. The optical properties and morphological surface structure of the thin films have been studied through techniques such as ultraviolet visible (UV-Vis), photoluminescence (PL), X-ray diffraction (XRD), and scanning electron microscopy (SEM).

## 2. Experimental

### 2.1. Materials

Manganese (II) acetate tetrahydrate, cyclohexamine, and salicylaldehyde were purchased from Sigma-Aldrich. Methanol, ethanol, acetone, and tetrahydrofuran (THF) were reagents purchased from Merck chemicals and were all used without further purification.

#### 2.1.1. Preparation of manganese complex

*Bis*(N-cyclohexyl-1-salicydenaminato)manganese(II) complex was prepared from the reaction of 10 mmol of 2-hydroxy-1-naphthaldehyde (20 mL) of ethanol with 10 mmol cyclohexamine (20 mL) ethanol and 5.0 mmol manganese (II) acetate tetrahydrate in a 250 mL one necked round bottom flask. The mixture was then stirred and refluxed at a temperature of 50 °C for 3 hrs. The precipitate was filtered, washed with ethanol, dried in a desiccator, weighed and characterized. *The manganese complex was obtained as a black solid, m.pt. 138 °C, CHN analysis: Anal. Calc. for  $\text{C}_{26}\text{H}_{32}\text{MnN}_2\text{O}_2$ : C, 67.95; H, 7.03; N, 6.14; O, 6.97. Found: C, 66.99; H, 6.80; N, 5.98; O, 6.60. Significant FTIR bands:  $\nu(\text{C}=\text{N})$ :  $1538\text{ cm}^{-1}$ ,  $\nu(\text{C}-\text{O})$ :  $1413\text{ cm}^{-1}$ ,  $\nu(\text{C}-\text{N})$ :  $1022\text{ cm}^{-1}$ ,  $\nu(\text{Mn}-\text{O})$ :  $548\text{ cm}^{-1}$ ,  $\nu(\text{Mn}-\text{N})$ :  $428\text{ cm}^{-1}$ .*

#### 2.1.2. Deposition of manganese oxide thin films by spin coating

Exactly, 0.15 g of *bis*(N-cyclohexyl-salicydenaminato)manganese(II) complex was dissolved in 20 mL of acetone in a small container. The solution was ultrasonicated to ensure a complete dissolution. The complex solution was then transferred on the 2 x 1.5 cm glass or silicon substrates which were previously washed with acetone using the spin coater which was rotated at 3000 rpm for 30 sec. After the deposition, the films were dried on a very low temperature hotplate for few minutes to remove the solvent and other organic residuals. The glass or silicon substrate with thin films were then annealed at various temperatures of 350, 450 and 550 °C for one hour inside the tube furnace under nitrogen gas environment.

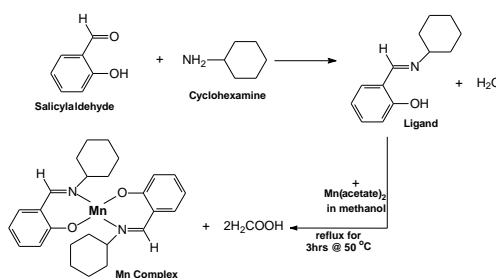
### 2.2. Physical measurements

Elemental Analyser: Elemental analysis of the precursor was achieved through a Perkin-Elmer automated model 2400 series II CHNS/O analyser. Fourier transform infrared spectroscopy: The FTIR spectrum of the precursor was done in the wavenumber range between 400–4000  $\text{cm}^{-1}$  through the utilization of a Bruker FTIR tensor 27 spectro-photometer. Thermogravimetric Analysis: A Perkin-Elmer Pyris 6 TGA was used for thermal analysis. A heating rate from 30 up to 900 °C was used in a closed perforated aluminium pan under nitrogen gas at a 20 °C  $\text{min}^{-1}$ . UV-Vis and Photoluminescence spectroscopy: Absorption measurements of the manganese oxide thin films were carried out using a Perkin-Elmer Lambda 1050 UV/vis/NIR spectrometer and the Edinburgh Instruments FLS920 spectrofluorimeter was used to investigate the luminescence

properties of the films. The thin films were measured using the glass or silicon clean slide as a reference. X-ray diffraction: X-ray diffractograms were recorded from a Bruker AXS D8 diffractometer using Cu-K $\alpha$  radiation where the samples were set flat and scanned between  $2\theta = 30\text{--}80^\circ$  in steps of  $0.05^\circ$  at a scan rate of 0.1 steps per second. Scanning electron microscopy: The surface morphology of the prepared films was observed using Philips XL-30 FEG scanning electron microscope. Films were first coated with carbon using Edwards E306A coating system.

### 3. Results and discussion

The preparation of manganese oxide thin films through the decomposition of *bis*(*N*-cyclohexyl-1-salicydenaminato)manganese(II) complex using spin coater at various temperatures is reported. The manganese precursor was obtained as shown in Scheme 1 below:



Scheme 1. The preparation of the *bis*(*N*-cyclohexyl-1-salicydenaminato)manganese(II) complex.

#### 3.1. Spectroscopic and Thermal studies of the manganese complex

Fourier transform infrared spectroscopy was used to disclose the chemical information and major functional groups of the materials. Fig. 1(a) shows the FTIR spectrum of the *bis*(*N*-cyclohexyl-1-salicydenaminato)manganese(II) complex which was conducted in the range of  $4000\text{--}400\text{ cm}^{-1}$ . The broad band was observed at  $3205\text{ cm}^{-1}$  which is ascribed to the symmetric stretching vibrational mode of hydroxyl groups in the solvent that was used for washing the complex. The peaks between  $2930\text{--}2335\text{ cm}^{-1}$  can be assigned to  $\text{--C--H}$  peaks from the benzene ring. The strong bands were observed at  $1538$ ,  $1413$ , and  $1022\text{ cm}^{-1}$  which were attributed to  $\text{C=N}$  group of the imine, phenolic  $\text{C--O}$  and  $\text{C--N}$ . The two strong and narrow absorption peaks at  $548$  and  $428\text{ cm}^{-1}$  were assigned to the pairing mode between nitrogen and oxygen to the metal ion (i.e.  $\text{Mn--O}$  and  $\text{Mn--N}$ ). Similar observation was reported by Ozkaya et al [30].

The thermal properties of *bis*(*N*-cyclohexyl-1-salicydenaminato)manganese(II) complex were studied with TGA-DTA technique. Fig. 1(b) shows the TGA/DTA curves of the precursor which was conducted under nitrogen atmosphere at the temperature ranging from  $20$  to  $900\text{ }^\circ\text{C}$ . The thermal analysis exhibited three decomposition steps weight loss. The first  $12\%$  weight loss between  $68\text{--}147\text{ }^\circ\text{C}$  is due to the evaporation  $\text{--OH}$  molecules from the solvent. The second partial weight loss of  $2\%$  between  $197\text{--}244\text{ }^\circ\text{C}$  maybe assigned to the decomposition of nitrates [31]. The third weight loss of  $39\%$  between  $197\text{--}244\text{ }^\circ\text{C}$  which was confirmed by DTA curve in dotted lines can be ascribed to the complete decomposition of some of the precursor constituents leaving manganese oxide.

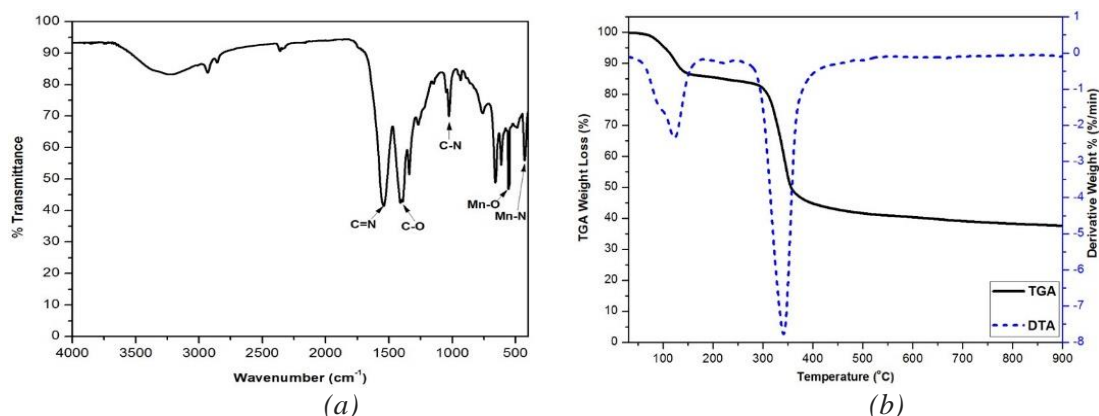


Fig. 1. FTIR spectrum (a) and TGA/DTA curves of bis(*N*-cyclohexyl-1-salicydenaminato) manganese(II) complex (b).

### 3.2. Optical properties

Fig. 2 shows the absorption spectra of the  $\text{Mn}_3\text{O}_4$  thin films prepared at 350, 450 and 550 °C on the glass and silicon substrates. The optical absorption spectra of the films prepared on the glass substrate illustrates the strong absorption bands at 455, 460, and 480nm whereas the films prepared on the silicon substrate exhibited well-defined peaks at 360, 365, and 375 nm which was increasing as the temperature was increased.

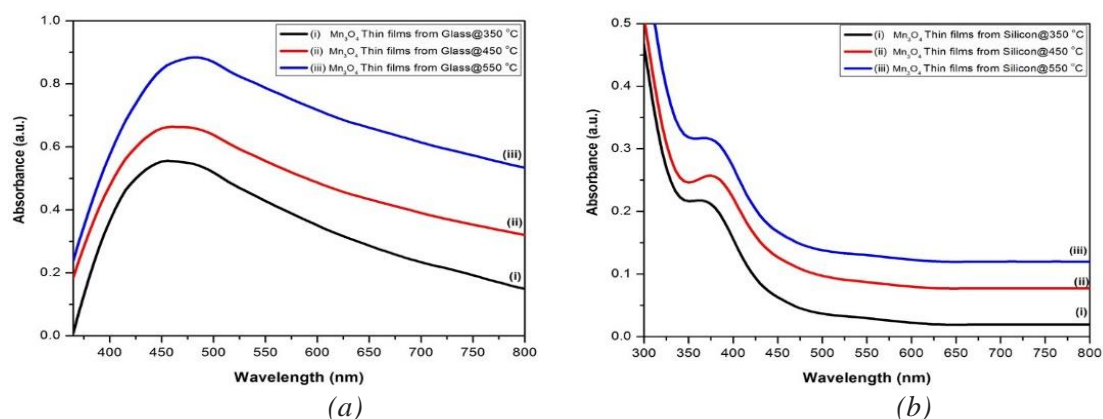


Fig. 2. Absorption spectra of manganese oxide thin films prepared with glass (a) and silicon (b) substrates at 350 (i), 450 (ii), and 550 °C (iii)

The optical band gap energies for the direct transition semiconductor material were assessed using Tauc's approach according to the following equation:

$$\alpha = \frac{A(h\nu - E_g)^{1/2}}{h\nu} \quad (1)$$

where  $A$  is a dimensional constant and  $E_g$  the optical band gap. The values of the optical band gap  $E_g$  were established by a linear extrapolation of the plot of  $(\alpha h\nu)^2$  against  $h\nu$  to the energy axis. It has been discovered that the optical band gap energies of the  $\text{Mn}_3\text{O}_4$  thin films were decreasing when the temperature was increased. The direct optical band gap energy of the films prepared on the glass substrate were found to be 1.34, 1.22 and 1.02 eV whereas the band gap energies prepared on the silicon substrates were located at 3.04, 2.85, and 2.74 eV. The deviations in optical band gap energy may be attributed to quantum confinements of the  $\text{Mn}_3\text{O}_4$  materials [32].

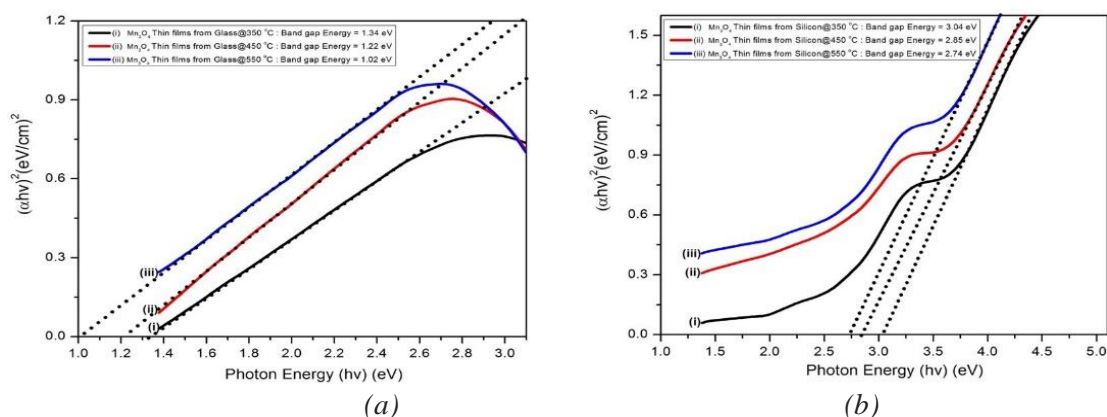


Fig. 3. Tauc plot of manganese oxide thin films prepared with glass (a) and silicon (b) substrates at 350 (i), 450 (ii), and 550 °C (iii)

Fig. 4 shows the emission spectra of the prepared  $\text{Mn}_3\text{O}_4$  thin films. The excitation at 500 nm exhibits the broad emission spectra with maximum intensities between 565 - 567 nm in the visible region along with the less intense vibrational shoulders, centred between 577 - 578 nm for all the prepared films. It has been observed that the emission spectra shift towards the higher wavelength as the preparation temperature was increased. The strong emission peaks imply the high crystalline character of the material [33].

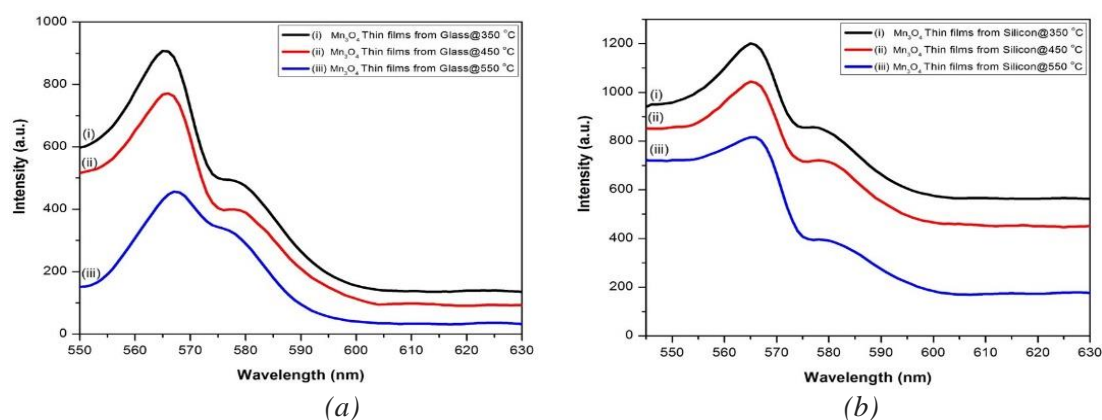


Fig. 4. Emission spectra of manganese oxide thin films prepared with glass (a) and silicon (b) substrates at 350 (i), 450 (ii), and 550 °C (iii)

### 3.3. Structural properties

X-ray diffraction (XRD) is an effective and a reliable technique used to determine crystal structure of a material. The corresponding XRD patterns of the prepared manganese oxide thin films from glass and silicon substrates are shown in Fig. 5. XRD patterns of all the prepared films displayed the peaks around 29.90, 32.66, 36.23, 37.83, 43.98, 50.88, 56.55, 58.64, 60.12, and 64.67° corresponding to (112), (103), (211), (004), (220), (105), (303), (321), (224), and (314) planes which could be easily indexed to the hausmannite  $\text{Mn}_3\text{O}_4$  tetragonal structure with JCPDS card no. 18-0803 with the lattice parameters  $a = b = 5.75 \text{ \AA}$  and  $c = 9.44 \text{ \AA}$  which were found to be in good agreement with the reported values [34, 35].

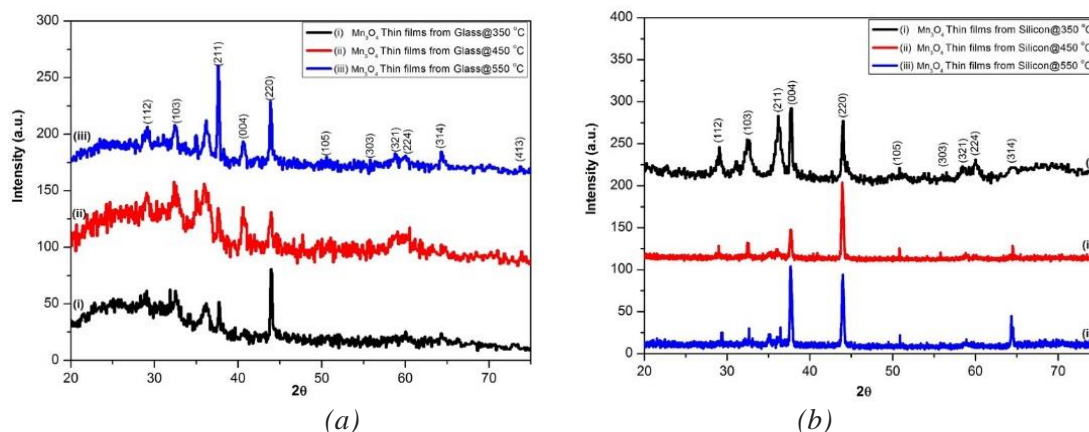


Fig. 5. X-ray diffraction patterns of manganese oxide thin films prepared with glass (a) and silicon (b) substrates at 350 (i), 450 (ii), and 550 °C (iii).

The surface morphology of the synthesized  $\text{Mn}_3\text{O}_4$  thin films have been studied via the scanning electron microscope in Fig. 6. The SEM image of the film prepared at lower temperatures in Fig. 6(i) shows the fatigue patterns on the glass surface with cracks whereas Fig. 6(iv) reveals cauliflower-like nanostructures. The SEM images (Fig. 6(ii) & (v)) of the films prepared at 450 °C displayed homogeneous, uniform and well covered surface on both substrates. Fig. 6(v) of the film prepared on silicon substrate further revealed a rough surface with a good particle packing and highly monodisperse spherical-like particles with diameter of ca. 41 nm. A further increase in annealing temperature to 550 °C projected the formation of large clustered particles in Fig. 6(iii). The SEM images of the film prepared on the silicon substrate (Fig. 6(vi)) showed the particles that were beginning to melt and form fluid like particles.

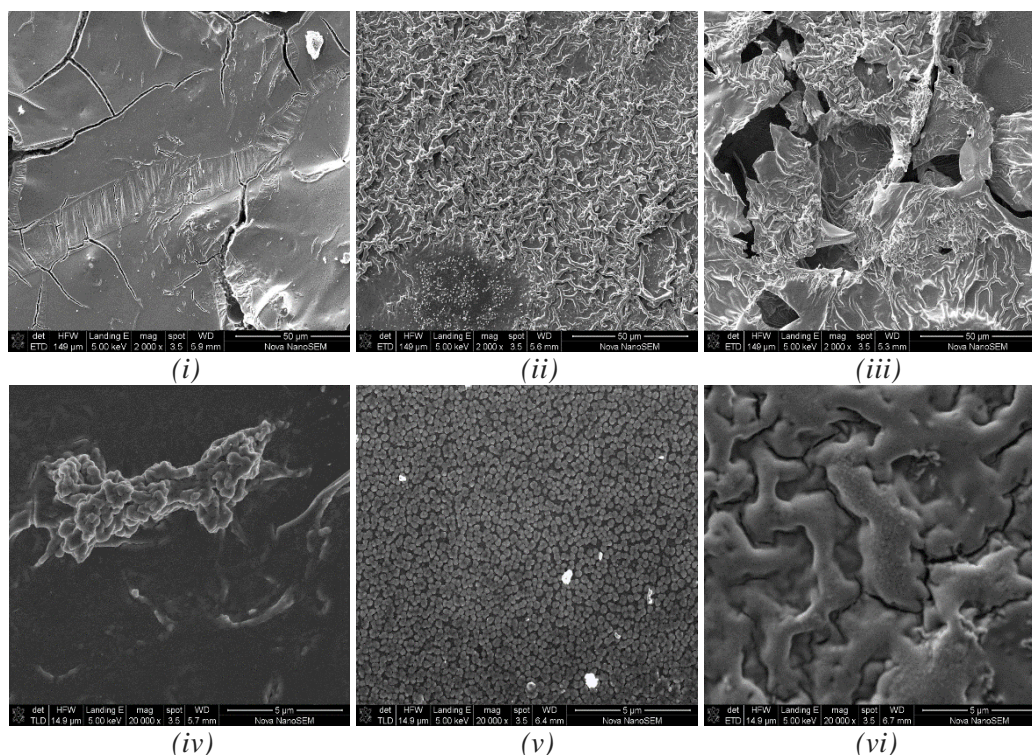


Fig. 6. SEM micrograms of manganese oxide thin films prepared with glass at 350 (i), 450 (ii) & 550 °C (iii) and silicon substrates at 350 (iv), 450 (v) & 550 °C (vi).

#### 4. Conclusions

In the present work, the preparation of *bis*(N-cyclohexyl-salicydenaminato)manganese(II) complex and the synthesis of Mn<sub>3</sub>O<sub>4</sub> thin films at various temperatures and on different substrates has been successfully accomplished. The absorption spectra of the films prepared on the silicon substrate revealed distinctive peaks between 360 - 375 nm. The optical band gap energies of the Mn<sub>3</sub>O<sub>4</sub> films prepared on the glass and silicon substrates were decreasing as the decomposition temperatures were increasing. The XRD patterns of all the Mn<sub>3</sub>O<sub>4</sub> thin films exhibited tetragonal structured nanocrystals. The SEM micrographs of the films displayed an improve in surface coverage with well-shaped particles when the temperature was increased.

#### Acknowledgements

Authors would like to extend their appreciation to the National Research Foundation (NRF) (Thuthuka Grant Holder no: TTK170508230117) and the Vaal University of Technology for funding this project.

#### References

- [1] M. Cho, J.-H. Seo, D.-W. Park, W. Zhou, Z. Ma, Appl. Phys. Lett. **108**, 233505 (2016).
- [2] V. E. Babicheva, A. Boltasseva, A. V. Lavrinenko, Nanophotonics **4**, 165 (2015).
- [3] T. Chen, M.-H. Wang, H.-P. Zhang, Z.-Y. Zhao, T.-T. Liu, Mater. Des. **96**, 329 (2016).
- [4] B. Ammundsen, J. Paulsen, Adv. Mater. **13**, 943 (2001).
- [5] J. D. Lee, Concise Inorganic Chemistry, fourth ed., Chapman-Hall, London, 734 (1991).
- [6] S. E. Fendorf, R. J. Zasoski, Environ. Sci. Technol. **26**, 79 (1992).
- [7] Y. Chabre, J. Pannetier, Solid State Chem. **23**, 1 (1995).
- [8] I. Espinal, S. L. Suib, J. F. Rusling, J. Am. Chem. Soc. **126**, 7676 (2004).
- [9] M. Tsuji, S. Komarneni, Y. Tamaura, M. Abe, Mater. Res. Bull. **27**, 741 (1992).
- [10] X. Hao, J. Zhao, Y. Li, Y. Zhao, D. Ma, L. Li, Colloids Surf. A **374**, 42 (2011).
- [11] M. Wu, Q. Zhang, H. Lu, A. Chen, Solid State Ion. **169**, 47 (2004).
- [12] C. N.R. Rao, A. K. Cheetham, Adv. Mater. **9**, 1009 (1997).
- [13] K. J. Kim, Y. R. Park, J. Cryst. Growth **270**, 162 (2004).
- [14] A. Ramírez, D. Friedrich, M. Kunst, S. Fiechter, Chem. Phys. Lett. **568–569**, 157 (2013).
- [15] S. Xing, Z. Zhou, Z. Ma, Y. Wu, Mater. Lett. **65**, 517 (2011).
- [16] M. L. Singla, S. Awasthi, A. Srivastava, Sens. Actut. B **127**, 580 (2007).
- [17] E. Machefaux, A. Verbaere, D. Guyomard, J. Power Sources **157**, 443 (2006).
- [18] M. Baldi, E. Finocchio, F. Milella, G. Busca, Appl. Catal. B: Environ. **16**, 43 (1998).
- [19] S. C. Pang, M. A. Anderson, T. W. Chapman, J. Electrochem. Soc. **147**, 444 (2000).
- [20] O. Nilsen, H. Fjellvag, A. Kjekshus, Thin Solid Films **444**, 44 (2003).
- [21] L. Ren, S. Wu, M. Yang, W. Zhou, S. Li. J. Appl. Phys. **114**, 53907 (2013).
- [22] C. C. Hu, T. W. Tsou, Electrochem. Commun **4**, 105 (2002).
- [23] S. Isber, E. Majdalani, M. Tabbal, T. Christidis, K. Zahraman, B. Nsouli, Thin Solid Films **517**, 1592 (2009).
- [24] D. P. Dubal, D. S. Dhawale, R. R. Salunkhe, V. J. Fulari, C. D. Lokhande, J. Alloy Compd. **497**, 166 (2010).
- [25] Y. Dai, K. Wang, J. Zhao, J. Xie, J. Power Sources **161**, 737 (2006).
- [26] O. Y. Gorbenko, I. E. Graboy, V. A. Amelichev, A. A. Bosak, A. R. Kaul, B. Guttler, V. L. Svetchnikov, H. W. Zandbergen, Solid State Commun. **124**, 15 (2002).
- [27] H. Y. Xu, S. Xu, H. Wang, H. Yan, J. Electrochem. Soc. **152**, C803 (2005).
- [28] M. R. Catalano, G. Malandrino, Physics Procedia **46**, 118 (2013).
- [29] D. W. Schubert and T. Dunkel, Spin-Coating, J. Appl. Phys. **49**, 3993 (2003).
- [30] T. Ozkaya, A. Baykal, H. Kavas, Y. Koseoglu, M. S. Toprak, Physica B **403**, 3760 (2008).

- [31] T. Xaba, B. W. Masinga, M. J. Moloto, Digest Journal of Nanomaterials and Biostructures **11**, 123116).
- [32] M. Sittishoktram, E. Ketsombun, T. Jutarosaga, J. Phys.: Conf. Ser. **901**, (2017) 12099.
- [33] T. Xaba, M. J. Moloto, O. Nchoe, Z. Nate, N. Moloto, Chalcogenide Letters **14**, 337 (2017).
- [34] J. Bhagwan, A. Sahoo, K. L. Yadav, Y. Sharma, Electrochimica Acta **174**, 992 (2015).
- [35] J. Duan, Y. Zheng, S. Chen, Y. Tang, M. Jaroniec, S. Qiao, Chem. Commun. **49**, 7705 (2013).